Chapter 2

Synthesis, characterization and preformulation of lisofylline

1. Introduction

As discussed in the previous chapter, our objective is to design hydrophobic prodrug of LSF and delivering the same using micelles based nanoformulation. However, before beginning with the formulation of LSF, preformulation data including the relevant physiochemical and biopharmaceutical properties of LSF that are of paramount significance to determine the appropriate formulation and delivery strategy was collected.[1] The drug was synthesized and characterized *in house* considering the high market expense of this drug (LSF >99% pure, 25 mg > Rs.14,000 in Sigma Aldrich, India and Cayman chemicals, USA). The drug synthesized in our lab was found to be >98% pure and very cost effective (5 gm, ~Rs. 10,000). LSF is a less explored drug in literature and no experimental physiochemical properties are reported; we also did not come across any of its formulations. In this chapter, physiochemical and biopharmaceutical properties of LSF including metabolism of LSF from PTX, its interconversion issues & challenges associated with LSF delivery and its current status in diabetes as well as in other auto immune diseases shall be discussed.

2. Materials and methods

2.1. Materials and reagents

PTX (purity ≥99%) was purchased from Tokyo Chemical Industry Pvt. Ltd. (TCI, Mumbai India). Methanol (HPLC grade), diethyl ether and dichloromethane (DCM; extra pure) were obtained from Merck (Mumbai, India). Sodium chloride (NaCl), potassium bromide and sodium borohydride ($NaBH_4$) were purchased from SRL Pvt. Ltd. (Mumbai, India). $CDCl_3$ was purchased from Sigma Aldrich (USA). All other chemicals and reagents were of analytical grade and used as obtained.

2.2. Lisofylline: Synthesis and characterization

2.2.1. Synthesis of LSF

LSF was synthesized by reduction of its parent molecule, PTX using $NaBH_4$ (**Figure 2.1**). PTX (1.00 g, 1 eq.) was dissolved in 50 mL of anhydrous methanol (extra pure) followed by portion wise addition of $NaBH_4$ (1.15 g, 2.5 eq); the mouth of the round bottom flask was not closed as addition of $NaBH_4$ evolves H_2 gas. The mixture was stirred for 12 hr at room temperature and the reaction was monitored by thin layer chromatography (TLC) (toluene/ acetone 1:1 v/v). The reaction solvent was evaporated under reduced pressure after completion of the reaction, and the residue was dissolved at DCM (100 mL). The organic layer was washed with saturated NaCl solution (brine; 2 × 80 mL), dried over anhydrous sodium sulphate (Na_2SO_4), filtrated using Whatman filter paper (No.1) and finally concentrated under reduced pressure. The residue was recrystallized from ice-cold diethyl ether to obtain white crystals of LSF (900 mg, 90% yield).

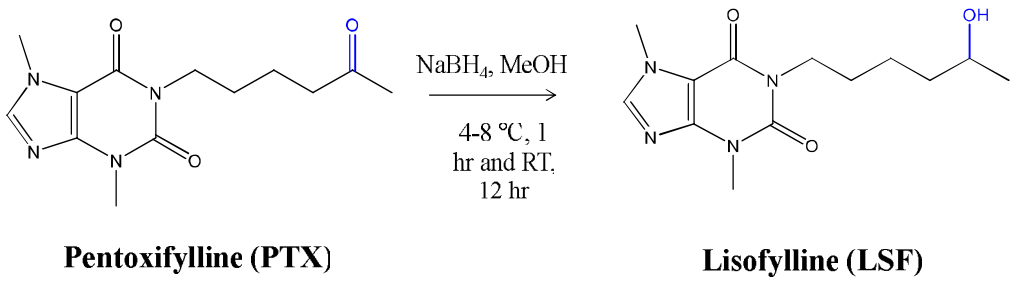

Pentoxifylline (PTX) **Lisofylline (LSF)**

Figure 2.1 Synthesis of LSF from PTX.

2.2.2. Characterization of synthesized LSF

Synthesized LSF was characterized by ^{1}H NMR, Fourier transform infra-red spectroscopy (FT-IR), mass spectrometry, HPLC and differential scanning calorimetry (DSC) **(Figure 2.2).** In ^{1}H NMR (**Figure 2.2A**), LSF showed a chemical shift at 3.75 (-CH-OH; f) corresponding to the

presence of hydroxyl group in the side chain of LSF which is formed owing to the reduction of keto group of PTX. For mass determination, high resolution mass spectrometry (HR-MS) analysis was carried out in ESI+ mode (**Figure 2.2B**). Expected mass of LSF by its molecular formula ($C_{13}H_{20}N_4O_3$) was calculated to be 280.1535 g/mol, mass analysis showed $(M+H)^+$ ion peak at m/z 281.161 (**Figure 2.2B**). Thus, the mass of LSF calculated by HR-MS was 280.1537 g/mol (281.161-1.0078 (Mass of ^1H) =280.1532). Purity of the final product was confirmed by high performance liquid chromatography (HPLC; **Table 2.1**). Purity of LSF was

Table 2.1
Liquid chromatographic conditions for purity analysis of LSF

	Analytical Method
HPLC	Shimadzu, Japan (Binary pump)
Column (SP)	Intersil® ODS(C18), 250× 4.6 mm, 5µ
Mobile Phase	Methanol : Water (65:35 % v/v)
Retention time (RT)	4.6 min for LSF
Run time	7 min
Flow rate	1 mL/min
LSF λmax	273 nm
Column temperature	RT
Injection volume	20 µL
Mode	Reverse Phase
Detector	PDA

found to be >98% (**Figure 2.2C**). Further confirmation was carried out using FT-IR, wherein, functional group region 4000-1400 cm^{-1} was analyzed, LSF showed –CH-OH frequency at 3400-3300 cm^{-1} (**Figure 2.2D**). DSC thermogram showed the melting point (**Figure 2.2E**) of LSF to be 124.45°C (123-125 °C). In the DSC thermogram, no melting peak corresponding to free PTX

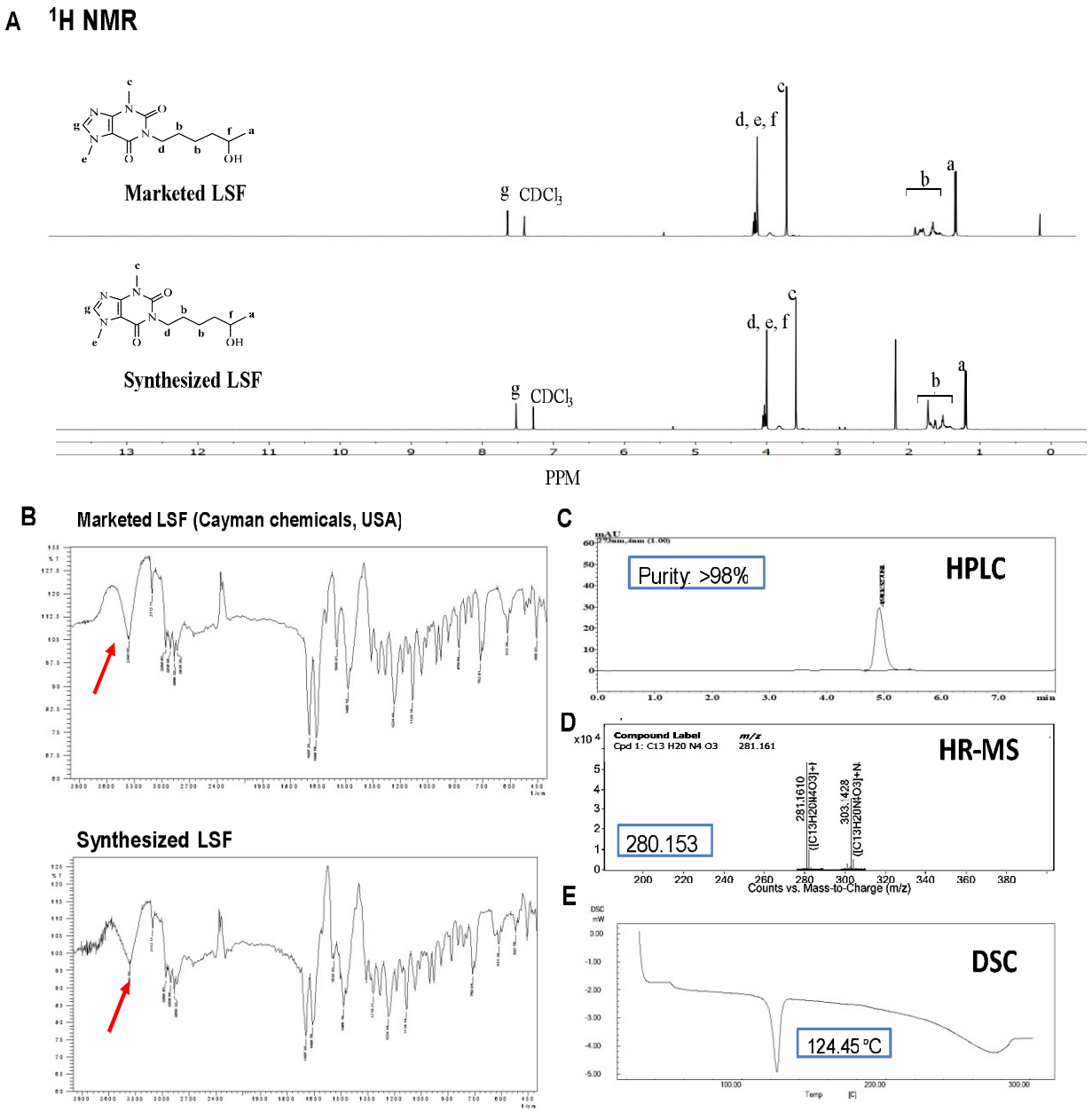

Figure 2.2. Characterization of synthesized LSF. (A) ^{1}H NMR ($CDCl_3$, 400 mHz), (B) FT-IR (arrow indicates characteristic –OH group stretch at 3360 cm^{-1}, (C) HPLC chromatogram for purity analysis (purity: >98%), (D) mass analysis using HR-MS (280.1532 g/mol) and, (E) melting point analysis by DSC (melting point: 124.45 °C).

(T_m: 103-105 ºC) was seen confirming that there was no free PTX present in the synthesized LSF.

3. Preformulation studies of LSF

Preformulation studies are designed to provide an insight into the essential physicochemical attributes of a drug which are of importance in designing a suitable dosage form of the drug.[2] Different physiochemical properties of LSF (PubChem CID: 501254) as reported in the literature are enlisted in **Table 2.2.**

3.1. Solubility studies

The pH dependent equilibrium solubility of LSF in aqueous buffers was performed by using shake flask method. For pH dependent solubility determination, different buffers in the pH range of 1.2 to 12 were prepared using buffer tables (I.P.). Saturated solutions of *in house* synthesized LSF were prepared in eppendorf tubes by adding an appropriate volume of selected aqueous media (water/buffers; typically in 0.2-0.25 mL) into each tube containing a known quantity of solid LSF (typically in the range 15-20 mg). The tubes were shaken for a predefined time period (24 h) at RT and then centrifuged at 17,000 rpm for 10 min and also filtered using PTFE-filters with 0.22 µm pore size. Filter absorption was avoided by discarding the first few drops of the filtrate. The amount of dissolved LSF was determined by UV spectroscopy (Jasco V750 spectrophotometer).

A pH dependent solubility profile of LSF is shown in **Figure 2.3.** As shown in **Figure 2.3A,** LSF did not exhibit pH dependent solubility (approx. 22-25 mg/mL). The aqueous solubility of *in house* synthesized LSF was found to be 23.8 ± 0.3 mg/mL which was found to be comparable to the marketed LSF (Cayman chemicals, USA) 24.93 ± 0.17 mg/mL at RT.

Further, to determine the maximum solubility of LSF at different pH values, samples of equilibrium solubility containing excess LSF were bath sonicated for 15 min × 4 cycles at RT

followed by centrifugation at 17,000 rpm for 10 min and filtered using PTFE-filters with 0.22 µm pore size. The amount of dissolved LSF was determined by UV spectroscopy. pH dependent maximum solubility of LSF is shown in **Figure 2.3B** wherein, it was observed that upon sonication, the solubility of LSF was enhanced by ~2 folds in the pH range 4-12 (approx. 40-46 mg/mL) while for pH values between 1-3, solubility was enhanced by 3 times than its equilibrium solubility (approx. 58-61 mg/mL). Sonication also increased the water solubility of LSF up to 2.5 folds (*in house* synthesized LSF vs. marketed LSF, 61.76 ± 0.45 mg/mL and 62.14 ± 1.07 mg/mL respectively) at RT.

Drug solubility in organic solvents is equally useful in drug product development processes such as formulation and bioanalytical method development. So, LSF solubility was also determined in commonly used organic solvents such as chloroform, dichloromethane, acetone, methanol, acetonitrile, ethanol, diethyl ether, 2-propanol, DMSO, dimethyl formamide (DMF), ethyl acetate and hexane. Among these solvents, LSF was highly soluble in chloroform and dichloromethane but very poorly soluble in hexane. (**Figure 2.3C**).

3.2. Partition co-efficient

Experimental partition coefficient (log P) was determined using shake-flask method using n-hexane-water system. For experiment, n-hexane and water in equal volume (10 mL) were kept for saturation for 24 h. After saturation of solvents, a known amount of LSF (10 mg) was added (n=4) and the resultant dispersion was placed in shaker water bath at 37 °C for 2 h for clear phase separation. Each phase sample was transferred to a 2.0 ml eppendorf tube and centrifuged at 17,000 rpm for 10 min and dissolved LSF was analyzed using UV spectroscopy. For, n-hexane, 1 mL solution was evaporated and reconstituted in water for LSF analysis. Log P was calculated using ratio of LSF concentration in organic phase (hexane) to concentration of LSF in

aqueous phase (water). The n-hexane-water system log P for LSF was found to be -0.96 ± 0.02 which indicated a very hydrophilic nature of LSF.

3.3. Dissociation constant

The dissociation constant (pKa) of a molecule is an important physicochemical parameter which has significant effect on its solubility, lipophilicity, permeability and protein binding. So, pKa of LSF was determined using UV spectroscopy.[3,4]

For pKa determination, LSF at 10 µg/mL concentration was prepared in different pH buffers ranging from 1.2 to 12. To estimate the wavelength of maximum absorption as a function of pH, absorption spectra was plotted from 200-400 nm for low, medium and high pH (1.2, 7 and 12) solutions. Afterwards, absorption maxima was estimated at 273 and 230 nm. At both the wavelengths, absorbance of LSF in buffers of different pH values was recorded and ratio of absorbance values was plotted against pH. The inflection point in the resultant curve was determined as the approximate pKa value of LSF and was found to be 4.3 (**Figure 2.3D**).

Table 2.2

Physiochemical properties of LSF

Parameters	Properties
IUPAC Name	5-Hydroxyhexyl-3,7-dimethylxanthine
Synonyms	Lysofylline, Hydroxy-pentoxifylline, Penthydroxifillyne
Density	1.3±0.1 g/cm^3
Boiling Point	511.2±56.0 °C at 760 mmHg
Melting Point	123-125ºC
Molecular Formula	$C_{13}H_{20}N_4O_3$
Molecular Weight	280.323 g/mol
Flash Point	263.0±31.8 °C
Exact Mass	280.153534
Appearance	solid | white
Index of Refraction	1.621
Storage condition	Refrigerator -20 °C

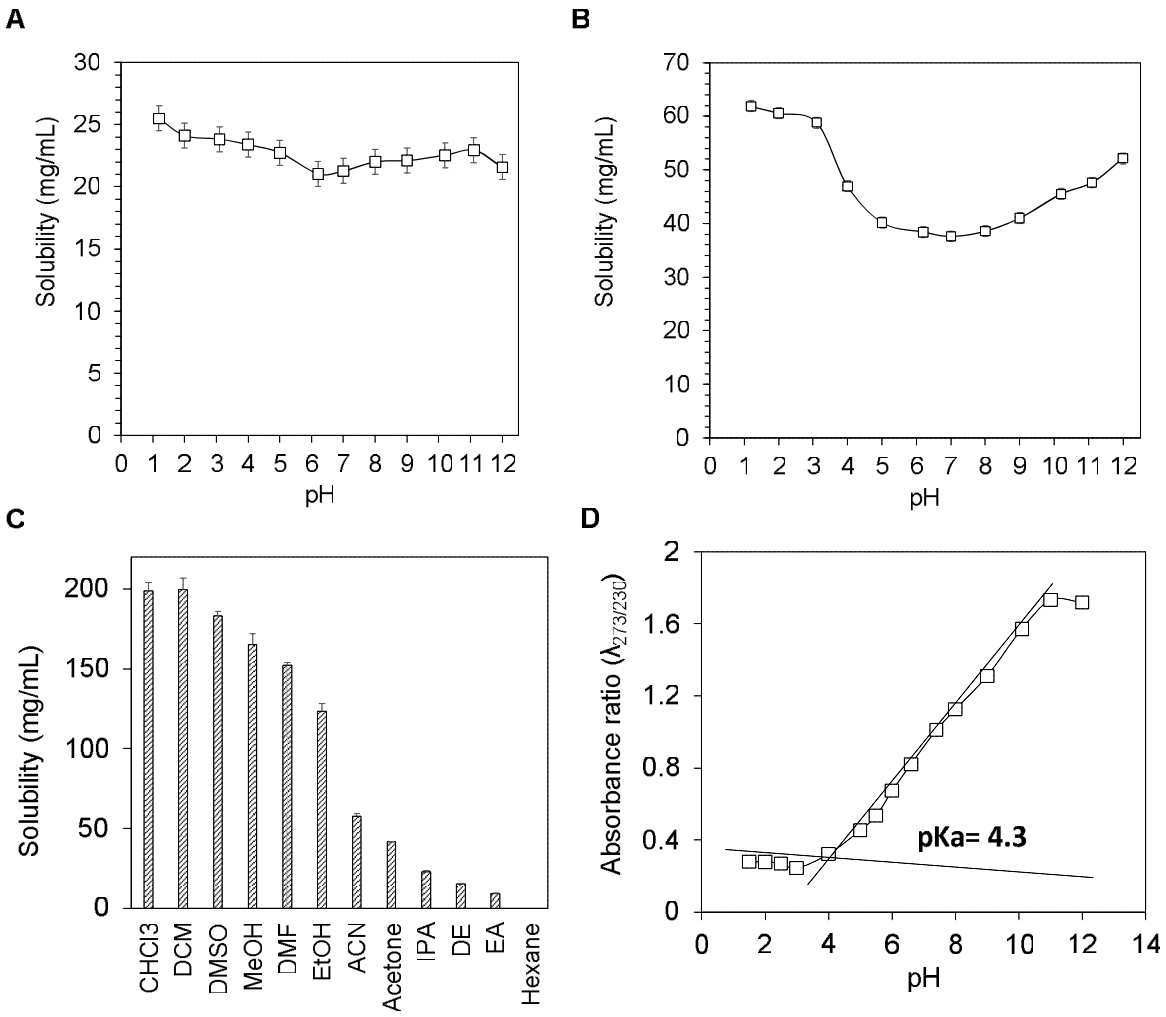

Figure 2.3. Solubility and pKa determination of LSF. pH dependant solubility profiles for (A) equilibrium solubility and, (B) maximum solubility (aided by sonication), (C) LSF solubility in different organic solvents and, (D) pKa determination curve using UV spectroscopy

Here, We could use data-set of absorption responses in a series of buffer solutions with different pH values, keeping the total concentration of our ionizing species constant (10 µg/ml in our experiment), in order to determine the pKa using UV-visible spectroscopy. But, this approach

can be problematic since small changes in concentration can introduce significant 'noise' in the data, making the position of the ionization of LSF in the absorption/ pH profile unclear.

To overcome this problem, we can normalize any differences in concentration by using the ratio of the absorption values at two different wavelengths which gives a response that is independent of concentration. LSF exhibited two peaks at 230 and 273 nm in its absorption spectra which show shifting due to ionization of LSF as a function of pH. So, we choose ratio of 273 and 230 nm to determine pKa value of LSF.

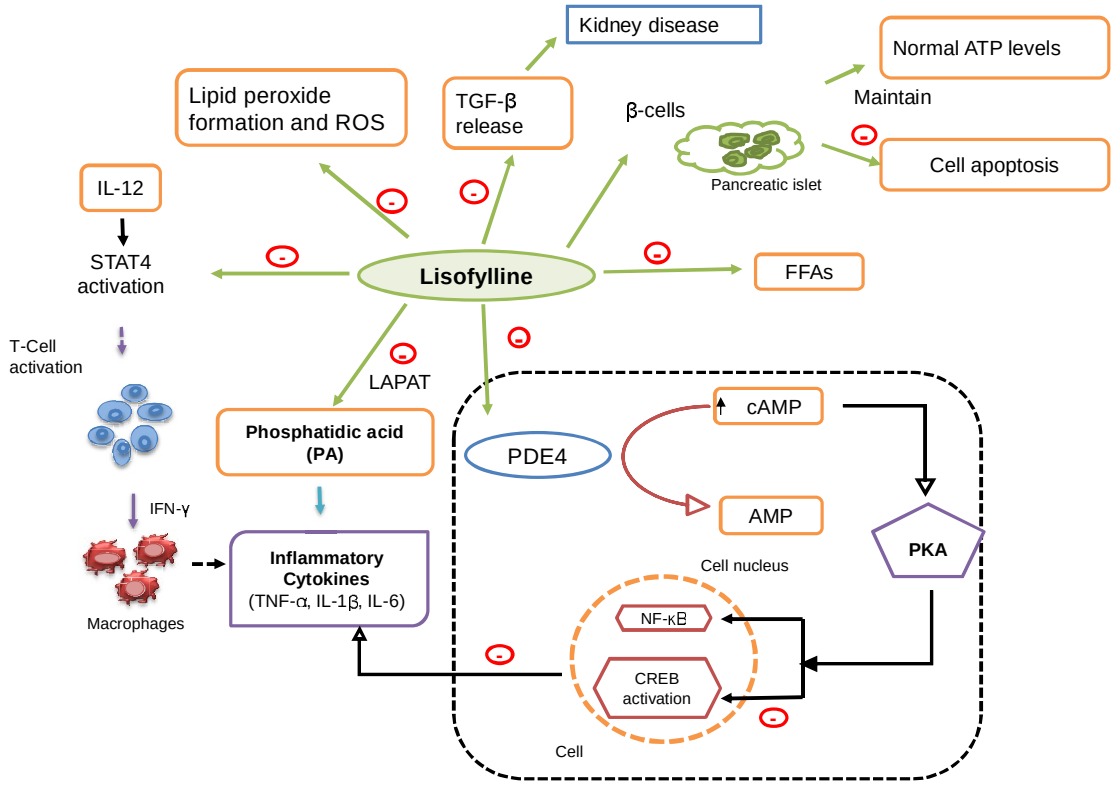

Figure 2.4. Possible immunological mechanisms of LSF

(LAPAT: Lysophosphatidate acyltransferase; PA: Phosphatidic acid; FFA: Free fatty acid; PDE4: Phosphodiesterase 4; PKA: Protein kinase A; CREB: cAMP response element binding protein; STAT4: Signal transducers and activators of transcription 4)

4. Mechanism of LSF therapeutic activity

The key mechanisms of activities demonstrated by LSF were not clearly known but probable mechanisms based on literature are shown in **Figure 2.4**. LSF mainly acts by inhibition of phosphodiesterase 4 (PDE4) enzymes.[5] An inhibition of these enzymes results in increased levels of intracellular cAMP and a subsequent phosphorylation of protein kinase A, leading to the phosphorylation of numerous transcription factors responsible for regulation of the production of inflammatory cytokines.[6] It is well known that PDE4 inhibitors reduce the release of pro-inflammatory cytokines and increase the production of certain anti-inflammatory cytokines, thus restoring the balance lost in inflammatory and autoimmune diseases.[7,8] Apart from that, LSF prevents hyperoxia-induced lung injury by inhibiting activation, membrane oxidation and pro-inflammatory cytokine production of the cAMP response factor binding protein (CREB).[9]

Potent pro-inflammatory mediators induce multiple and diverse biological responses across a wide variety of cell types.[10] The biological effects of these pro-inflammatory mediators are also significantly overlapping and redundant. Phosphatidic acid (PA) may be the second messenger that might have intracellular signaling functions, towards several proinflammatory stimuli- not clear.[11] Pro-inflammatory mediators such as tumor necrosis factor alpha (TNF-α), interleukin 1 beta (IL-1β), and endotoxins (lipopolysaccharide; LPS) rapidly induces intracellular PA species.[12,13] LSF inhibits generation of this PA thus suppressing the cell membrane-associated enzyme, lysophosphatidate acyltransferase (LPAT).[14] Reduction in PA formation and LPAT activity could suppress host response to TNF-α and IL-1β in inflammatory reaction.[15] LSF has demonstrated a marked protective effect in a variety of acute inflammatory diseases such as acute lung injury and acute respiratory distress syndrome in preclinical studies that may be attributed to the inhibition of this shared second messenger pathway involving PA. [5,16,17]

Signal transducer inhibitor and transcription (STAT4) factor plays a prominent role in the regulation of systemic immune response. The STATs are a family of latent cytosolic transcription factors, including STAT1, STAT2, STAT3, STAT4, STAT5a, STAT5b and STAT6.[18,19] Following the binding of cytokines or growth factors to their receptors, STAT proteins can be phosphorylated on either tyrosine or serine residues for activation.[20] STAT4 is expressed in activated peripheral blood monocytes, dendritic cells (DC) and macrophages at sites of inflammation in humans.[21] STAT4 mediates IL-12 signaling that is critical for the development of protective immunity in intracellular infection. Interruption of the STAT4 gene results in suppression of T cell activation and reduction of T cell-driven cytokine production.[22,23] LSF blocks IL-12 biological actions, reduces IFN-γ production and regulates T cell differentiation and activation.[21,23,24] Due to the interruption in IL-12 signaling, LSF activity has been recognized in mouse allergic encephalomyelitis (EAE), an experimental model of multiple sclerosis. [15,25] Therefore, LSF could be clinically useful for immune regulation and prophylactic therapy for autoimmune disorders.

The immune cells, including T cells, B cells, macrophages, dendritic cells, and NK cells, as well as cytokines contribute to up-regulation of the Th1-type responses, leading to pancreatic cell destruction.[26] Since activated T cells directly cause cytotoxicity in β cells, IL-12 may directly and indirectly facilitate the development of Type 1 diabetes.[27,28] An excessive amount of IFN-γ is detected in islets during the progression of diabetes in humans and animals. Experimental observations suggest that IFN-γ and TNF-α inhibit insulin secretion in isolated islets and cell lines.[29-31] Blocking the expression or the function of these cytokines by LSF has shown to slow down the development of T1DM in rodent models.[32,33]

In addition, LSF can maintain normal mitochondrial membrane potential and ATP levels and block apoptosis induced by inflammatory cytokines.[34] LSF also blocks lipid peroxide formation and reactive oxygen species (ROS), in addition to having antioxidant and free radical scavenging properties.[35,36] For diabetic complication, LSF has been shown to reduce TGF-β release from bone marrow cells.[34] Given the emerging information on the role of mitochondria and ROS in the progression of diabetic complications, anti-inflammatory agents that protect mitochondria and reduce downstream inflammatory cascades could provide a new way of preventing or retarding diabetes complications such as renal damage.

LSF also causes a rapid and prolonged suppression of serum levels of free fatty acids (FFA) in humans. A reduction in total FFA and unsaturated FFA in serum, might be relevant to the anti-inflammatory activity of LSF, and might serve as a surrogate pharmacodynamic marker of the compound, since total FFA and unsaturated FFA are increased in patients of after trauma or sepsis comparison to levels in healthy subject.[37] LSF inhibits stress-activated lipid metabolic pathways in human studies and suppresses the circulating levels of the linoleic acid, hydroperoxyl, and hydroxyocatadecadienic acid oxidation products.[38]

5. Metabolism of PTX to LSF and interconversion of LSF to PTX

Metabolic pathways of PTX and its metabolite LSF are depicted in **Figure 2.5.**[39] LSF is an active metabolite of PTX but under *in vivo* conditions shows the tendency to again convert into PTX that is LSF and PTX undergo interconversion.[40] Main sites of PTX metabolism and interconversion are reported to be erythrocytes (having carbonyl reductase), lung clara cells (having pulmonary carbonyl reductase) and liver microsomes. PTX forms a total of 7 metabolites, among these, metabolite 1 (LSF) is found to be active in diabetes as well as other autoimmune diseases. Cytochromes (CYPs), CYP1A2, CYP2E1 and CYP3A4 are primarily involved in LSF and PTX

metabolism/interconversion and are mainly found in liver. Former two CYPs are mainly responsible for metabolism of PTX to LSF while the latter CYP is responsible for LSF metabolism and coverts LSF to metabolite 3 (**Figure 2.5**). This interconversion of LSF is mainly attributed to the presence of free hydroxyl group in the side chain of LSF. LSF-PTX interconversion leads to a high dose and frequent dosing of LSF.[40]

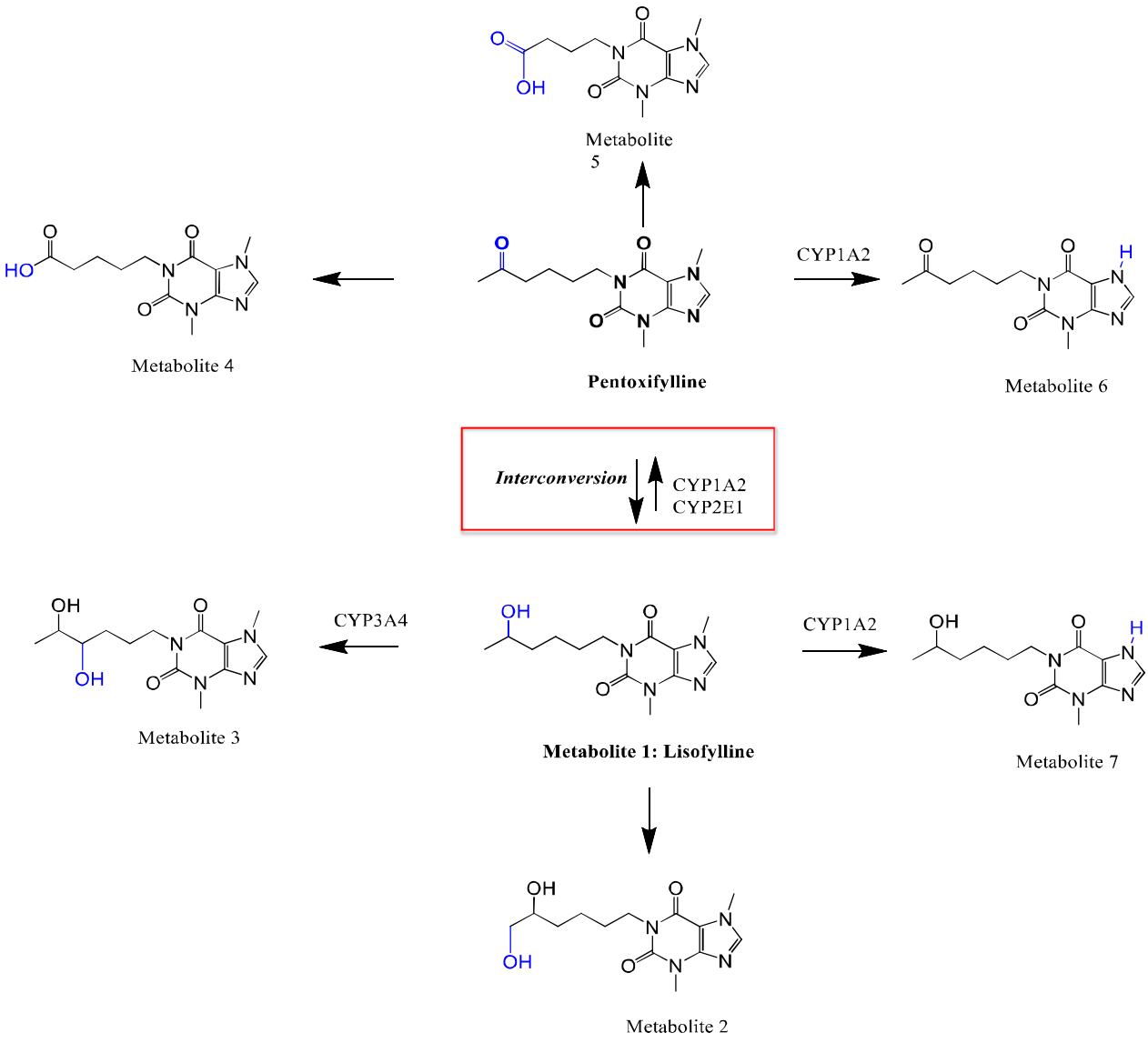

Figure 2.5. Metabolic pathway of PTX and its metabolite LSF

6. Conclusion

LSF was successfully synthesized by $NaBH_4$ reduction method with 90% yield and characterized with different spectroscopic and chromatographic techniques. Further, study of its physiochemical and biopharmaceutical properties reflect the challenges associated with LSF delivery. However, literature also exemplifies the therapeutic value of LSF in several autoimmune diseases (such as T1DM, endotoxemia, hepatitis, arthritis etc.) and thus a suitable delivery system is needed to harness its potential.

Bibliography

1. Desu, P. K.; Vaishnavi, G.; Divya, K.; Lakshmi, U. An overview on preformulation studies. *Indo American Journal of Pharmaceutical Sciences* **2015,** *2*, (10), 1399-1407.

2. Acharya, P. C.; Shetty, S.; Fernandes, C.; Suares, D.; Maheshwari, R.; Tekade, R. K., Preformulation in Drug Research and Pharmaceutical Product Development. In *Dosage Form Design Considerations*, Elsevier: 2018; pp 1-55.

3. Pandey, M.; Jaipal, A.; Kumar, A.; Malik, R.; Charde, S. Determination of pKa of felodipine using UV–Visible spectroscopy. *Spectrochimica Acta Part A: Molecular and Biomolecular Spectroscopy* **2013,** *115*, 887-890.

4. Dai, L.-L.; Zhang, H.-Z.; Nagarajan, S.; Rasheed, S.; Zhou, C.-H. Synthesis of tetrazole compounds as a novel type of potential antimicrobial agents and their synergistic effects with clinical drugs and interactions with calf thymus DNA. *MedChemComm* **2015,** *6*, (1), 147-154.

5. Świerczek, A.; Wyska, E.; Baś, S.; Woyciechowska, M.; Mlynarski, J. PK/PD studies on non-selective PDE inhibitors in rats using cAMP as a marker of pharmacological response. *Naunyn-Schmiedeberg's archives of pharmacology* **2017,** *390*, (10), 1047-1059.

6. Bischoff, E. Potency, selectivity, and consequences of nonselectivity of PDE inhibition. *International journal of impotence research* **2004,** *16*, (1), S11-S14.

7. Lagente, V.; Martin-Chouly, C.; Boichot, E.; Martins, M. A.; Silva, P. M. Selective PDE4 inhibitors as potent anti-inflammatory drugs for the treatment of airway diseases. *Memórias do Instituto Oswaldo Cruz* **2005,** *100*, 131-136.

8. Jankowska, A.; Swierczek, A.; Chlon-Rzepa, G.; Pawlowski, M.; Wyska, E. PDE7-selective and dual inhibitors: advances in chemical and biological research. *Current medicinal chemistry* **2017,** *24*, (7), 673-700.

9. George, C. L.; Fantuzzi, G.; Bursten, S.; Leer, L.; Abraham, E. Effects of lisofylline on hyperoxia-induced lung injury. *American Journal of Physiology-Lung Cellular and Molecular Physiology* **1999,** *276*, (5), L776-L785.

10. Rahmati, M.; Mobasheri, A.; Mozafari, M. Inflammatory mediators in osteoarthritis: A critical review of the state-of-the-art, current prospects, and future challenges. *Bone* **2016,** *85*, 81-90.

11. Jones, P. Development of second generation epigenetic agents. *MedChemComm* **2012,** *3*, (2), 135-161.

12. Pokotylo, I.; Kravets, V.; Martinec, J.; Ruelland, E. The phosphatidic acid paradox: too many actions for one molecule class? Lessons from plants. *Progress in lipid research* **2018,** *71*, 43-53.

13. Bursten, S.; Weeks, R.; West, J.; Le, T.; Wilson, T.; Porubek, D.; Bianco, J. A.; Singer, J. W.; Rice, G. C. Potential role for phosphatidic acid in mediating the inflammatory responses to TNF alpha and IL-1 beta. *Circulatory shock* **1994,** *44*, (1), 14-29.

14. Bleich, D.; Chen, S.; Bursten, S. L.; Nadler, J. L. Lisofylline, an inhibitor of unsaturated phosphatidic acid generation, ameliorates interleukin-1 beta-induced dysfunction in cultured rat islets. *Endocrinology* **1996,** *137*, (11), 4871-4877.

15. Oka, Y.; Hasegawa, N.; Nakayama, M.; Murphy, G. A.; Sussman, H. H.; Raffin, T. A. Selective downregulation of neutrophils by a phosphatidic acid generation inhibitor in a porcine sepsis model. *Journal of Surgical Research* **1999,** *81*, (2), 147-155.

16. Świerczek, A.; Wyska, E.; Pociecha, K.; Baś, S.; Mlynarski, J. Influence of inflammatory disorders on pharmacokinetics of lisofylline in rats: implications for studies in humans. *Xenobiotica* **2019,** *49*, (10), 1209-1220.

17. Świerczek, A.; Pociecha, K.; Ślusarczyk, M.; Chłoń-Rzepa, G.; Baś, S.; Mlynarski, J.; Więckowski, K.; Zadrożna, M.; Nowak, B.; Wyska, E. Comparative Assessment of the New PDE7 Inhibitor–GRMS-55 and Lisofylline in Animal Models of Immune-Related Disorders: A PK/PD Modeling Approach. *Pharmaceutical Research* **2020,** *37*, (2), 1-21.

18. Juczynska, K.; Wozniacka, A.; Waszczykowska, E.; Danilewicz, M.; Wągrowska-Danilewicz, M.; Zebrowska, A. Expression of JAK3, STAT2, STAT4, and STAT6 in pemphigus vulgaris. *Immunologic Research* **2020**, 1-7.

19. Yang, Z.; Chen, M.; Ellett, J. D.; Fialkow, L. B.; Carter, J. D.; McDuffie, M.; Nadler, J. L. Autoimmune diabetes is blocked in Stat4-deficient mice. *Journal of autoimmunity* **2004,** *22*, (3), 191-200.

20. Stark, G. R.; Cheon, H.; Wang, Y. Responses to cytokines and interferons that depend upon JAKs and STATs. *Cold Spring Harbor perspectives in biology* **2018,** *10*, (1), a028555.

21. Ferreli, C.; Lai, C.; August, S.; Buggy, Y.; Kumar, P.; Brownlow, N.; Parker, P.; Friedmann, P. S.; Ardern-Jones, M.; Pickard, C. STAT 4 expression and activation is increased during mitosis in vitro and in vivo in skin-and mucosa-derived cell types: implications in neoplastic and inflammatory skin diseases. *Journal of the European Academy of Dermatology and Venereology* **2017,** *31*, (10), 1663-1673.

22. Sawant, D. V.; Yano, H.; Chikina, M.; Zhang, Q.; Liao, M.; Liu, C.; Callahan, D. J.; Sun, Z.; Sun, T.; Tabib, T. Adaptive plasticity of IL-10+ and IL-35+ T reg cells cooperatively promotes tumor T cell exhaustion. *Nature immunology* **2019,** *20*, (6), 724-735.

23. Wyska, E.; Świerczek, A.; Pociecha, K.; Przejczowska-Pomierny, K. Physiologically based modeling of lisofylline pharmacokinetics following intravenous administration in mice. *European journal of drug metabolism and pharmacokinetics* **2016,** *41*, (4), 403-412.

24. YANG, Z.; CHEN, M.; FIALKOW, L. B.; Ellett, J. D.; WU, R.; NADLER, J. L. Inhibition of STAT4 activation by lisofylline is associated with the protection of autoimmune diabetes. *Annals of the New York Academy of Sciences* **2003,** *1005*, (1), 409-411.

25. Bright, J. J.; Du, C.; Coon, M.; Sriram, S.; Klaus, S. J. Prevention of experimental allergic encephalomyelitis via inhibition of IL-12 signaling and IL-12-mediated Th1 differentiation: an effect of the novel anti-inflammatory drug lisofylline. *The Journal of Immunology* **1998,** *161*, (12), 7015-7022.

26. Chang, J. H.; Jiang, Y.; Pillarisetty, V. G. Role of immune cells in pancreatic cancer from bench to clinical application: an updated review. *Medicine* **2016,** *95*, (49).

27. Campbell-Thompson, M.; Fu, A.; Kaddis, J. S.; Wasserfall, C.; Schatz, D. A.; Pugliese, A.; Atkinson, M. A. Insulitis and β-cell mass in the natural history of type 1 diabetes. *Diabetes* **2016,** *65*, (3), 719-731.

28. Pirot, P.; Cardozo, A. K.; Eizirik, D. L. Mediators and mechanisms of pancreatic beta-cell death in type 1 diabetes. *Arquivos Brasileiros de Endocrinologia & Metabologia* **2008,** *52*, (2), 156-165.

29. Wachlin, G.; Augstein, P.; Schröder, D.; Kuttler, B.; Klöting, I.; Heinke, P.; Schmidt, S. IL-1β, IFN-γ and TNF-α increase vulnerability of pancreatic beta cells to autoimmune destruction. *Journal of autoimmunity* **2003,** *20*, (4), 303-312.

30. Fathy, S. A.; Mohamed, M. R.; Ali, M. A.; EL-Helaly, A. E.; Alattar, A. T. Influence of IL-6, IL-10, IFN-γ and TNF-α genetic variants on susceptibility to diabetic kidney disease in type 2 diabetes mellitus patients. *Biomarkers* **2019,** *24*, (1), 43-55.

31. Fatima, N.; Faisal, S. M.; Zubair, S.; Ajmal, M.; Siddiqui, S. S.; Moin, S.; Owais, M. Role of pro-inflammatory cytokines and biochemical markers in the pathogenesis of type 1 diabetes: correlation with age and glycemic condition in diabetic human subjects. *PloS one* **2016,** *11*, (8).

32. Italiya, K. S.; Mazumdar, S.; Sharma, S.; Chitkara, D.; Mahato, R. I.; Mittal, A. Self-assembling lisofylline-fatty acid conjugate for effective treatment of diabetes mellitus. *Nanomedicine: Nanotechnology, Biology and Medicine* **2019,** *15*, (1), 175-187.

33. Striffler, J. S.; Nadler, J. L. Lisofylline, a novel anti-inflammatory agent, enhances glucose-stimulated insulin secretion in vivo and in vitro: studies in prediabetic and normal rats. *Metabolism* **2004,** *53*, (3), 290-296.

34. Bolick, D. T.; Hatley, M. E.; Srinivasan, S.; Hedrick, C. C.; Nadler, J. L. Lisofylline, a novel antiinflammatory compound, protects mesangial cells from hyperglycemia-and angiotensin II-mediated extracellular matrix deposition. *Endocrinology* **2003,** *144*, (12), 5227-5231.

35. Bhat, V. B.; Madyastha, K. Antioxidant and radical scavenging properties of 8-oxo derivatives of xanthine drugs pentoxifylline and lisofylline. *Biochemical and Biophysical Research Communications* **2001,** *288*, (5), 1212-1217.

36. Sturm, A.; Zeeh, J.; Sudermann, T.; Rath, H.; Gerken, G.; Dignass, A. U. Lisofylline and lysophospholipids ameliorate experimental colitis in rats. *Digestion* **2002,** *66*, (1), 23-29.

37. Bursten, S. L.; Federighi, D.; Wald, J.; Meengs, B.; Spickler, W.; Nudelman, E. Lisofylline causes rapid and prolonged suppression of serum levels of free fatty acids. *Journal of Pharmacology and Experimental Therapeutics* **1998,** *284*, (1), 337-345.

38. Husain, A.; Rosales, N.; Schwartz, G. K.; Spriggs, D. R. Lisofylline Sensitizes p53 Mutant Human Ovarian Carcinoma Cells to the Cytotoxic Effects ofcis-Diamminedichloroplatinum (II). *Gynecologic oncology* **1998,** *70*, (1), 17-22.

39. Wyska, E. Pharmacokinetic interaction between verapamil and methylxanthine derivatives in mice. *Drug metabolism letters* **2010,** *4*, (1), 15-24.

40. Wyska, E.; Pękala, E.; Szymura, O., Joanna. Interconversion and tissue distribution of pentoxifylline and lisofylline in mice. *Chirality* **2006,** *18*, (8), 644-651.